Center for International and Security Studies at Maryland

Requirements and Feasibility for the Transition from a Ballistic Missile Capability to an Anti-Satellite (ASAT) Capability

Jaganath Sankaran

December 2007

UNIVERSITY OF MARYLAND

CISSM
School of Public Policy
4113 Van Munching Hall
University of Maryland
College Park, MD 20742
Tel: 301-405-7601
cissm@umd.edu

This paper was prepared as part of the Advanced Methods of Cooperative Security Program at the Center for International and Secuirty Studies at Maryland, with generous support from the John D. and Catherine T. MacArthur Foundation.

Abstract

Ballistic missiles and anti-satellite (ASAT) weapons operate using similar technological means but not with the same level of technology or engineering maturity. ASATs require more sophisticated systems engineering and integration requirements to adapt to the challenges posed by an ASAT intercept. The main difficulties arise from the requirements for detection in space and the high closing velocities needed to execute an ASAT intercept [1]. These difficulties have been underestimated after the recent Chinese ASAT test by those who have suggested that other nations could in the near-future master this technology gap and convert their primitive ballistic missile capabilities into an effective ASAT weapons capability.

This report examines whether Iran could use its modest missile capability to project a viable ASAT threat to US Low-Earth Orbit (LEO) satellites. The study suggests that, even if Iran has an Intermediate Range Ballistic Missile (IRBM), it would not be easily able to leap-frog the technology gap from a ballistic missile to an ASAT capability. Unless it develops and tests the system vigorously and visibly, Iran would not project an ASAT threat.

Chapter 1 of the report analyzes the capability of the Iranian Shahab-4 missile, including the velocity attained by the missile at an altitude of 1000 kilometers. Chapter 2 provides an analysis of the total thermal energy emitted by a model satellite in the Infrared (IR) band of interest for the given ASAT characteristics. Using the total thermal energy in the IR band, the detection range from which the ASAT can lock on to the satellite is determined. Chapter 3 details both, the ideal and real-time Proportional Navigation Guidance (PNG) law simulation performed using the parameters obtained in Chapters 1 and 2. The miss distances and acceleration requirements are shown graphically to capture the nuances and limits in the capability of an ASAT based on current Iranian technology level. The conclusion explains the limits and assumptions of this analysis and scope for further work.

Acknowledgements

A previous version of this working paper served as the practicum report for my Master of Engineering and Public Policy degree and was completed under the supervision of Dr. Nancy Gallagher and Dr. David Wright. Support for this project was provided by the John D. and Catherine T. MacArthur Foundation.

Chapter 1

Missile Capability

In the analysis undertaken for this study, a three stage missile, the Iranian Shahab-4 is taken as the baseline anti-satellite weapon. This missile is used as the baseline since it is the most advanced missile that Iran is presumed to possess. The capability of the missile and the altitude that it can attain when launched vertically on a path into space as opposed to against a target in earth are ascertained using the Rocket equations.

1.1 The Rocket Equation for Multiple Stages

The rocket equation is given by

$$\Delta V_1 = -V_{e_1} ln(\frac{m_{final_1}}{m_{initial_1}}) = -V_{e_1} ln(r_1) \tag{1.1}$$

where ΔV_1 is the total change in velocity imparted to the rocket body using the propellant of the first stage after the first stage burnout. Similarly

$$\Delta V_2 = -V_{e_2} ln(r_2) \tag{1.2}$$

Assuming $V_{e_1} = V_{e_2} = V_e$

$$\Delta V_1 + \Delta V_2 = -V_e ln(r_1) - V_e ln(r_2) = -V_e ln(r_1 r_2). \tag{1.3}$$

Now ΔV for multistage rockets is

$$\Delta V_{tot} = \sum_{k=1}^{n\ \ stages} \Delta V_k = \sum_{k=1}^{n\ \ stages} V_{e,k} ln(\frac{m_{initial,k}}{m_{final,k}}) \tag{1.4}$$

where

$$m_{initial,k} = m_{payload} + m_{propellant,k} + m_{inert,k} + \sum_{j=k+1}^{n} (m_{propellant,j} + m_{inert,j}) \tag{1.5}$$

$$m_{final,k} = m_{payload} + m_{inert,k} + \sum_{j=k+1}^{n} (m_{propellant,j} + m_{inert,j}) \tag{1.6}$$

and

$$V_e = I_{sp} g \tag{1.7}$$

Using equation 1.4 the total ΔV capability or lift capacity and altitude attained can be determined.

1.2 Shahab-4 or IRSL X-2

The satellite launch version of the Shahab-4 is called the IRSL X-2. IRSL X-2 is used in this study as the launch vehicle for the Anti-satellite (ASAT) weapon. It is a Taepodong-1 missile with a third stage and satellite (as payload) added. The technical characteristics of the Taepodong-1 based IRSL X-2 are listed in table 1.1 below [9]. Iran has attempted to use this vehicle to launch satellites, albeit without success.

Table 1.1: Parameters of *Shahab* 4

Diameter	$0.8 - 1.3\ m$
Height	$25\ m$
Launch Weight	$22,000\ kg$
Thrust	$26,000\ kg - f$
Burn Time	$293\ s$
Stages	$2, 3$
Fuel	$Heptyl$
Oxidiser	$RFNA$
Third Stage	$SolidMotor$
Payload	$50 - 100\ kg$

1.3 ΔV Capability of IRSL X-2

The first stage of the IRSL X-2 is the No-dong missile, the second stage is a modified SCUD-B, and the third stage is a solid motor. The various stage parameters are detailed in tables 1.2, 1.3 and 1.4 [9].

1.3.1 Stage-1 (No-dong)

The characteristics of the first stage are listed in table 1.2. The ΔV of the first stage is determined using equation 1.4 and the respective dry and wet masses of the stages.

Table 1.2: Stage-1 parameters of IRSL X-2

Height	$approx.\ 14\,m\ with\ inter-stage\ truss\ sturcture$
Diameter	$1.32\ to\ 1.35\,m$
Launch Weight	$15,100\,kg$
Thrust (Actual)	$31,260\,kg-f$
Isp	$230\,s\ at\ sea\ level$
Burn Time	$95\,s$
Fuel	$TM-185\ (20\ percent\ gasoline\ +\ 80\ percent\ Kerosene)$
Oxidiser	$AK-27I\ (27\ percent\ N_2O_4\ +\ 73\ percent\ HNO_3\ +\ Inhibitor)$
Propellant Mass	$12,912\,kg$

$$m_{initial} = 15,100\,kg + 5,770\,kg + 1,000\,kg = 21,870\,kg \tag{1.8}$$

$$m_{final} = 21,870 - 12,912 = 8,958\,kg \tag{1.9}$$

$$V_e = g * I_{sp} = 9.81(230) = 2256\,m/s \tag{1.10}$$

Using the rocket equation the ΔV of the first stage is

$$\Delta V_{1^{st}Stage} = -V_e ln(\frac{m_{final}}{m_{initial}}) = 2014\,m/s \tag{1.11}$$

1.3.2 Stage-2 (SCUD-B)

The characteristics of the second stage are listed in table 1.3. In a similar fashion to the previous calculations the ΔV of the second stage is determined using equation 1.4 and the respective dry and wet masses of the stages 2 and 3 and payload weight.

Table 1.3: Stage-2 parameters of IRSL X-2

Height	$10\ m$
Diameter	$0.88\ m$
Launch Weight	$5,260\ to\ 5,770\ kg$
Thrust	$6,690 - 7,523\ kg - f\ at\ 50 - 55\ percent\ thrust$
Burn Time	$< 171\ s$
Fuel	$TM - 185\ (20\ percent\ gasoline\ +\ 80\ percent\ Kerosene)$
Oxidiser	$AK - 27I\ (27\ percent\ N_2O_4\ +\ 73\ percent\ HNO_3\ +\ Inhibitor)$

$$m_{initial} = 5,770\ kg + 1,000\ kg = 6,770\ kg \tag{1.12}$$

Assuming that 86 percent of the initial weight is propellant weight

$$m_{propellant} = 0.86(6,770) = 5822\ kg \tag{1.13}$$

hence

$$m_{final} = 6,770 - 5822 = 948\ kg \tag{1.14}$$

$$V_e = g * I_{sp} = 9.81(230) = 2256\ m/s \tag{1.15}$$

$$\Delta V_{2^{nd}stage} = -V_e ln(\frac{m_{final}}{m_{initial}}) = 4436\ m/s \tag{1.16}$$

1.3.3 Stage-3 (Solid Motor)

The characteristics of the second stage are listed in table 1.4. The ΔV of the third stage is determined using equation 1.4 and the mass of the third stage and payload weight.

$$m_{initial} = 1,000\,kg \tag{1.17}$$

Let

$$m_{final} = payload\ \ weight = 200\,kg \tag{1.18}$$

Assuming the I_{sp} of the solid motor propellant to be 200 s,

$$V_e = I_{sp} * g = 200(9.81) = 1962\,m/s \tag{1.19}$$

Thus,

$$\Delta V_{3^{rd}stage} = 3158\,m/s \tag{1.20}$$

Table 1.4: Stage-3 Solid Motor parameters of IRSL X-2

Height	$1\ \ or\ \ 2\,m$
Diameter	$0.65\,m$
Launch Weight	$approx.\ 550 - 1000\,kg\ \ total\ \ package$

1.4 Total ΔV capability of missile

$$\Delta V_{tot} = \Delta V_{1^{st}stage} + \Delta V_{2^{nd}stage} + \Delta V_{3^{rd}stage} \tag{1.21}$$

$$\Delta V_{tot} = 2014 + 4436 + 3158 = 9608\,m/s. \tag{1.22}$$

A simulation was run with this total ΔV capability to determine the altitude the missile can reach and the velocity at an assumed intercept altitude of $1000\,km$. The simulation was run using initial simplifying assumptions

of an impulsive missile, a flat-earth and non-rotating earth model, zero-drag and constant gravity with respect to altitude.

$$Maximum\ \ Altitude\ \ for\ \ given\ \ \Delta V_{tot} = 4703\, km \tag{1.23}$$

$$Velocity\ \ of\ \ missile\ \ at\ \ 1000\, km = 8528\, m/s. \tag{1.24}$$

Using the velocity of the missile at 1000 km the capability of the missile to execute an ASAT intercept at the altitude can be studied thereby providing a model for evaluation of the missile's ASAT capabilities.

Chapter 2

Temperature and Thermal Signature of Satellite

An important parameter in executing an ASAT intercept is the ability of the missile to map and image the thermal signature of the satellite. This function is directly dependent on the imaging sensors employed by the ASAT missile. This chapter analyzes this particular capability of the IRSL X-2 to mount such an imaging system on their missile systems.

A model LEO satellite is selected for the purpose of this study. The dimensions of the satellite were taken from the NASA Imager for Magnetosphere-to-Aurora Global Exploration (IMAGE) satellite [7]. The shape of the satellite is a octagonal cylinder with the following parameters.

$$Diameter = 237\,cm \approx 2.4\,m \tag{2.1}$$

$$Width\ \ of\ \ each\ \ face = 90\,cm = 0.9\,m \tag{2.2}$$

$$Height\ \ of\ \ each\ \ octagonal\ \ face = 136\,cm \approx 1.4\,m \tag{2.3}$$

The surface area of the eight faces of the octagon are

$$= 8 * (0.9 * 1.4) = 10\,m^2 \tag{2.4}$$

The surface area of the top and bottom octagonal surfaces is determined by diving the surfaces of the octagon into eight isosceles triangles with base of 90 cm and two equal sides of 118.5 cm (the radius of the octagon). Using

the Pythagorean theorem, the height of each triangle is found to be 110 cm. Thus the surface area of each isosceles triangle is

$$= (1/2 * 110 * 90) = 4950\, cm^2 \approx 0.5\, m^2 \tag{2.5}$$

The area of both the octagonal surfaces is

$$= 2 * 8 * 0.5 = 8\, m^2 \tag{2.6}$$

Thus the total surface area of the satellite is

$$= 10 + 8 = 18\, m^2 \tag{2.7}$$

2.1 Temperature of Satellite in Low Earth Orbit (LEO) Facing the Sun

For an object in thermal equilibrium in space,

$$P_E = P_A + P_I \tag{2.8}$$

where P_E is the power emitted by the object, P_A is the power absorbed by the object, and P_I is any power generated internally by the object.

$$P_E = A_s \varepsilon_{IR} \sigma T^4 \tag{2.9}$$

$$P_A = A_c \left[(S + S_R)\alpha_V + \alpha_{IR} E\right] \tag{2.10}$$

where A_s and A_c are the surface area and average cross-sectional area of the satellite, ε_{IR} is the emissivity averaged over the the IR band, σ is the Stefan-Boltzmann constant, S is the solar flux, S_R is the solar flux reflected from the earth (albedo flux= $0.3S$), E is the earth infrared flux (about $240\, W/m^2$), α_V is the satellite absorptivity averaged over the visible and near infrared band, and α_{IR} is the satellite absorptivity averaged over the IR band. For this calculation, the power internally generated is assumed as

$$P_I = 100\, W \tag{2.11}$$

For the given satellite

$$A_s = 18\, m^2 \tag{2.12}$$

To determine average cross-sectional area A_c, it is assumed that the top and bottom surfaces of the satellite are pointed in a direction perpendicular

to the sun and earth and that the side surfaces are facing the sun and earth. Therefore, the average cross-sectional area is the projected surface area of the satellite facing the sun which is rectangular surface with the width (i.e. diameter) and height of the octagonal satellite

$$A_c = 2.4 * 1.4 = 3.4\, m^2 \tag{2.13}$$

$$S = 1360\, W/m^2 \tag{2.14}$$

$$S_R = 0.3S = 408\, W/m^2 \tag{2.15}$$

$$E = 240\, W/m^2 \tag{2.16}$$

$$Assuming\ \varepsilon_{IR} = \alpha_{IR} = 0.8 \tag{2.17}$$

and

$$\alpha_V = 0.2 \tag{2.18}$$

For the satellite in thermal equilibrium,

$$A_s \varepsilon_{IR} \sigma T^4 = A_c \left[(S + S_R)\alpha_V + \alpha_{IR} E\right] + P_I \tag{2.19}$$

$$18 * 0.8 * 5.67 * 10^{-8} * T^4 = 3.4\left[1360(1.3)0.2 + 0.8(240)\right] + 100 \tag{2.20}$$

Hence the temperature of the satellite in LEO facing the sun is

$$T = 221\ K \tag{2.21}$$

2.2 Temperature of Satellite in Low Earth Orbit(LEO) in Earth's Shadow

In earth's shadow

$$P_A = A_c \alpha_{IR} E \tag{2.22}$$

For thermal equilibrium

$$A_s \varepsilon_{IR} \sigma T^4 = A_c \alpha_{IR} E + P_I \tag{2.23}$$

Hence the temperature of the satellite in LEO in earth's shadow is

$$T = 174\ K \tag{2.24}$$

2.3 Total Thermal Energy Emitted by the Satellite in the $4 - 5\mu.m$

This analysis assumes that Iran would have access to a Indium Antimonide (InSb) kind of array for IR detection. Although these arrays have a theoretical wavelength detection range from $2\,\mu.m$ to $6\,\mu.m$, their actual operating range is restricted to $4\,\mu.m$ to $5\,\mu.m$ due to transmitting window characteristics and other practical issues. Therefore, the energy emitted is measured in the band of $4\,\mu.m$ to $5\,\mu.m$.

The total emissive power of a black body is given by

$$E_b = \sigma T^4 \tag{2.25}$$

where σ, the Stefan-Boltzmann constant is $5.67 * 10^{-8}\, W/m^2.K^4$

Thus the corresponding total emissive power when the satellite is in sunlight is

$$E_1 = \sigma * 221^4 = 135\, W/m^2 \tag{2.26}$$

and the total emissive power when the satellite is in Earth's shadow is

$$E_2 = \sigma * 174^4 = 52\, W/m^2 \tag{2.27}$$

2.3.1 Total Thermal Energy when Satellite is Sunlit

If $\lambda_1 = 4\,\mu.m$ and $\lambda_2 = 5\,\mu.m$ then

$$\lambda_1 T = 4(221) = 884\,\mu.m - K \tag{2.28}$$

and the corresponding black body radiating function is given as

$$F_{0\to\lambda_1} = 0.0001441 \tag{2.29}$$

The black body radiating function is determined through standard tables that are derived from integration of Stefan-Boltzmann Law. For a prescribed temperature and the wavelength interval from 0 to λ, this fraction is determined by the ratio of the energy in the band to the total energy under the black body emission curve [5].

$$F_{0\to\lambda} \equiv \frac{\int_0^\lambda E_{\lambda,b} d\lambda}{\int_0^\infty E_{\lambda,b} d\lambda} = \frac{\int_0^\lambda E_{\lambda,b} d\lambda}{\sigma T^4} = \int_0^{\lambda T} \frac{E_{\lambda,b}}{\sigma T^5} d(\lambda T) = f(\lambda T) \tag{2.30}$$

Since the integrand $(\frac{E_{\lambda,b}}{\sigma T^5})$ is exclusively a function of the wavelength-temperature product λT, the above integral may be evaluated to obtain $F_{0\to\lambda}$ as a function of only λT. Following from this is

$$F_{\lambda_1\to\lambda_2} = \frac{\int_0^{\lambda_2} E_{\lambda,b}d\lambda - \int_0^{\lambda_1} E_{\lambda,b}d\lambda}{\sigma T^4} = F_{(0\to\lambda_2)} - F_{(0\to\lambda_1).} \tag{2.31}$$

Therefore

$$\lambda_2 T = 5(221) = 1105\ \mu.m - K \tag{2.32}$$

and the corresponding black body radiating function is given as

$$F_{0\to\lambda_2} = 0.0013 \tag{2.33}$$

From this,

$$\Delta F = 0.0012 \tag{2.34}$$

hence the total energy (ϕ_T) in the $4-5\mu.m$ band is

$$\phi_T = 0.0012(E_1) = 0.0012(135) = 0.162\ W/m^2 \tag{2.35}$$

2.3.2 Total Thermal Energy when Satellite is in Earth's Shadow

If $\lambda_1 = 4\ \mu.m$ and $\lambda_2 = 5\ \mu.m$ then

$$\lambda_1 T = 4(174) = 696\ \mu.m - K \tag{2.36}$$

and the corresponding black body radiating function is given as

$$F_{0\to\lambda_1} = 7.68 * 10^{-6} \tag{2.37}$$

Similarly

$$\lambda_2 T = 5(174) = 870\ \mu.m - K \tag{2.38}$$

and the corresponding black body radiating function is given as

$$F_{0\to\lambda_2} = 0.000138 \tag{2.39}$$

From this,

$$\Delta F = 1.3032 * 10^{-4} \tag{2.40}$$

hence the total energy (ϕ_T) in the $4-5\ \mu.m$ band is

$$\phi_T = 1.3032 * 10^{-4}(E_1) = 1.3032 * 10^{-4}(52) = 0.007\ W/m^2 \tag{2.41}$$

Table 2.1: Total energy ϕ_T in $4-5\,\mu.m$ band

Temperature (K)	**Total energy (W/m^2)**	**Total Energy (W)**
221 (satellite - sunlit)	0.16	2.88
174 (satellite - earth's shadow)	0.07	1.26
250	0.73	13.14
300	6.00	108

2.4 Seeker Characteristics

It is assumed that Iran would use an InSb (Indium Antimonide) seeker to image the thermal signature of a satellite in LEO. Arrays of 256 $\times$ 256 configurations are commercially available. The parameters of this seeker are

$$D^*(@4.6\,\mu m) = 3.7 * 10^{12}\ \ Jones \tag{2.42}$$

operating temperature $= 77\,K$, effeciency $\eta = 90\ \ percent$, center to center spacing $= 30\,\mu m$, and operating wavelength range $= 4-5\,\mu m$.

2.4.1 Determination of Detection Range

The noise equivalent power (NEP) for the detector is given by [6]

$$NEP = \frac{(A_d * \beta)^{\frac{1}{2}}}{D^*} \tag{2.43}$$

where $A_d = 30 * 30\,\mu m^2$, and bandwidth is $\beta = 50\,Hz$. Hence NEP $= 5.73 * 10^{-15}\,W$. A Signal to noise (S/N) ratio of 13.6 dB (= 22.9) gives a 90 percent single-look probability of detection with a false alarm probability of 10^{-7}. Assuming that all the target (satellite) signal power (IR radiation) reaching the aperture of the seeker is focused onto a single detector element, then the power on the detector element is given by [6]

$$\phi_D = \frac{\phi_T A}{4\Pi R^2 L} \tag{2.44}$$

where A = optics aperture area, R = range to target, and L = system losses.

This power on the detector ϕ_D will be sufficient to detect the target if

$$\phi_D = (S/N)_{min} * NEP \tag{2.45}$$

where $(S/N)_{min}$ = S/N ratio required for detection, and NEP = the incident power that produces a signal equal to the average noise signal (that is, the NEP is the incident signal power that gives a signal-to-noise ratio of one).

$$\phi_D = 22.9 * 5.73 * 10^{-15} = 1.31 * 10^{-13}\ W \tag{2.46}$$

It is assumed here that the system losses are 20 percent (L = 1.2) and the diameter of the optical aperture is 10 cm.

$$r = \frac{10}{2} = 5\ cm \tag{2.47}$$

The optics aperture area is

$$A = \Pi r^2 = \Pi * \left(\frac{5}{100}\right)^2 = 7.85 * 10^{-3}\ m^2 \tag{2.48}$$

Thus the range to target [4] is determined by equation 2.44

$$R = \sqrt{\frac{\phi_T A}{(4\Pi L)\phi_D}} \tag{2.49}$$

Using this equation, the detection ranges (R) for various satellite temperatures in sunlight and earth's shadow conditions are determined and encapsulated in table 2.2.

Table 2.2: Detection Range

Temperature (K)	**Total energy (W)**	**Detection Range (Km)**
221 (satellite - sunlit)	2.88	107
173 (satellite - earth's shadow)	1.26	71
250	13.14	229
300	108	655

Using these detection range values a guidance simulation algorithm can be run to simulate the ASAT capability of the missile. This is done in the next chapter.

Chapter 3

Guidance Simulation

The intercept of the anti-satellite (ASAT) missile with a satellite is simulated with a Proportional Navigation Guidance (PNG) Law [8] using the 1000 km intercept altitude and the corresponding velocity estimated in chapter 1 along with the detection range estimated in chapter 2.

3.1 Proportional Navigation Guidance (PNG) Law

The proportional navigation guidance law issues acceleration commands, perpendicular to the instantaneous missile-satellite line-of-sight, which are proportional to the line-of-sight rate and closing velocity. The PNG law can be expressed as

$$n_c = N^{'} V_c \dot{\lambda} \tag{3.1}$$

where n_c is the acceleration command, $N^{'}$ is a unitless designer-chosen gain known as as the effective navigation ratio, V_c is the missile-satellite closing velocity, λ is the line-of-sight angle, and $\dot{\lambda}$ is the line-of-sight rate. In the current analysis where the missile uses IR, the line-of-sight is measured and closing velocity is estimated from the line-of-sight.

Figure 3.1 represents the engagement geometry. The missile, with velocity magnitude V_M, is heading at an angle L + HE with respect to the line of sight. The angle L is the missile lead angle. The lead angle is the theoretical correct angle for the missile to be on a collision course triangle with the satellite. In other words, if the missile is on a collision triangle, no further acceleration commands are required for the missile to hit the target. The

angle HE is the heading error, which represents the initial deviation of the missile from the collision triangle.

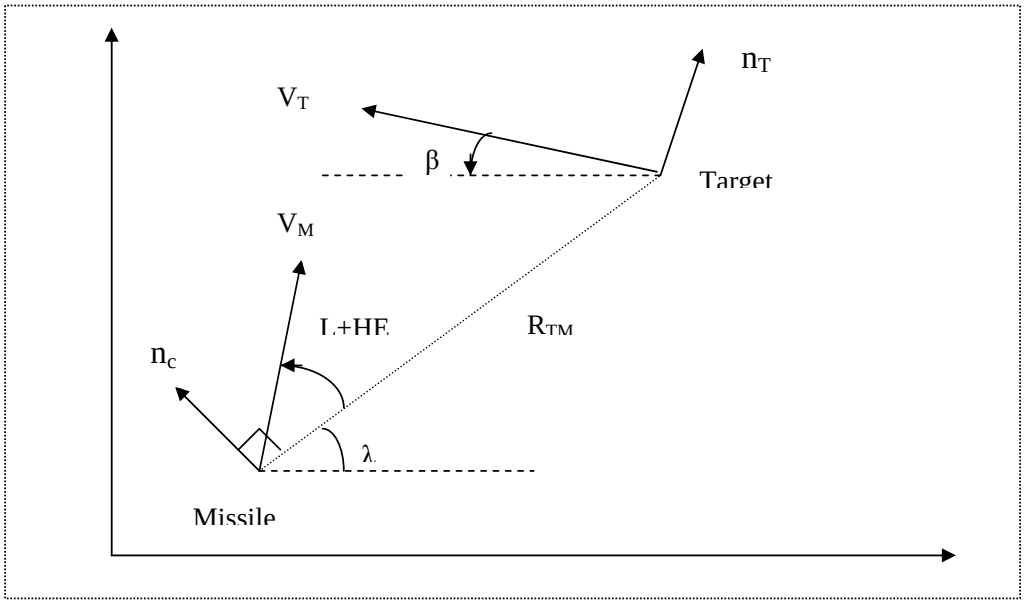

Figure 3.1: Two-dimensional missile-satellite engagement geometry [8]

The line connecting the missile and the satellite is the line-of-sight. The line-of-sight makes an angle λ with respect to the reference, and the length of the line-of-sight which is the instantaneous separation between the missile and the target satellite is denoted by R_{TM}. The point of closest approach of the missile and the satellite is known as the miss distance.

The closing velocity V_c is defined as the negative rate of change of the distance from the missile to the satellite

$$V_c = -\dot{R}_{TM} \tag{3.2}$$

Therefore, at the end of engagement, when the missile and target are in closest proximity, the sign of V_c will change. The closing velocity will be zero when R_{TM} is a minimum. The desired acceleration command n_c, which is derived from the proportional navigation guidance law, is perpendicular to the instantaneous line of sight.

In the simulated engagement model, the satellite can maneuver evasively with acceleration n_T. The target satellite acceleration is perpendicular to the target velocity vector; thus, the angular velocity of the satellite target is

expressed as

$$\dot{\beta} = \frac{n_T}{V_T} \tag{3.3}$$

where V_T is the satellite velocity. The components of the satellite velocity in the inertial coordinate system are found by integrating the differential equation for the flight path angle of the satellite, β, and substituting in

$$V_{T1} = -V_T cos\beta \tag{3.4}$$

$$V_{T2} = V_T Sin\beta \tag{3.5}$$

Satellite position components can be found by integrating the satellite velocity components. Therefore, the differential equations for the components of the target position are given by

$$\dot{R}_{T1} = V_{T1} \tag{3.6}$$

$$\dot{R}_{T2} = V_{T2} \tag{3.7}$$

Similarly the missile velocity and position differential equations are given by

$$\dot{V}_{M1} = a_{M1} \tag{3.8}$$

$$\dot{V}_{M2} = a_{M2} \tag{3.9}$$

$$\dot{R}_{M1} = V_{M1} \tag{3.10}$$

$$\dot{R}_{M2} = V_{M2} \tag{3.11}$$

where a_{M1} and a_{M2} are the missile acceleration.

The relative missile-satellite separations are

$$R_{TM1} = R_{T1} - R_{M1} \tag{3.12}$$

$$R_{TM2} = R_{T2} - R_{M2} \tag{3.13}$$

From figure 3.1 the line-of-sight is

$$\lambda = tan^{-1}\frac{R_{TM1}}{R_{TM2}} \tag{3.14}$$

If the relative velocity components in earth coordinates are defined as

$$V_{TM1} = V_{T1} - V_{M1} \tag{3.15}$$

$$V_{TM2} = V_{T2} - V_{M2} \tag{3.16}$$

we can calculate the line-of-sight rate by direct differentiation of the expression for the line-of-sight angle

$$\dot{\lambda} = \frac{R_{TM1}V_{TM2} - R_{TM2}V_{TM1}}{R_{TM}^2} \tag{3.17}$$

The relative separation between the missile and the satellite target, R_{TM}, can be expressed in terms of its inertial components by application of the distance formula, as

$$R_{TM} = \left(R_{TM1}^2 + R_{TM2}^2\right)^2 \tag{3.18}$$

Since the closing velocity is defined as the negative rate of change of the missile-satellite separation, it can obtained from differentiating equation 3.18

$$V_c = -\dot{R}_{TM} = \frac{-\left(R_{TM1}V_{TM1} + R_{TM2}V_{TM2}\right)}{R_{TM}} \tag{3.19}$$

The magnitude of the missile guidance command n_c can then be found by

$$n_c = N^{'}V_c\dot{\lambda} \tag{3.20}$$

Since the acceleration command is perpendicular to the instantaneous line-of-sight, the missile acceleration components can be found in earth coordinates

$$a_{M1} = -n_c sin\lambda \tag{3.21}$$

$$a_{M2} = n_c cos\lambda. \tag{3.22}$$

A missile employing PNG is not fired at the target but is fired in a direction to lead the target satellite. The initial angle of the missile velocity vector with respect to the line-of-sight is known as the missile lead angle L. The missile is fired at the expected intercept point. For the missile to be on a collision triangle, the theoretical missile lead angle is

$$L = sin^{-1}\frac{V_T sin(\beta + \lambda)}{V_M} \tag{3.23}$$

In actuality, the location of the intercept point can only be approximated since there is no prior knowledge of the target maneuver. Any angular deviation of the missile from the collision triangle is known as heading error HE. The initial missile velocity components can therefore be calculated as

$$V_{M1}(0) = V_M cos(L + HE + \lambda) \tag{3.24}$$

$$V_{M2}(0) = V_M sin(L + HE + \lambda). \tag{3.25}$$

3.2 Simulation with an idealized PNG-based ASAT

In simulating an idealized PNG-based ASAT, it is assumed that all the systems in the anti-satellite (ASAT) missile function as planned and required. A schematic of an idealized PNG law is shown in figure 3.2. In reality, the divert thrusters produce only one constant thrust level (either on or off) rather than a variable thrust, and the navigation system controls only their on-off pulse time. Thus, the control outputs are on-off commands and information about the pulse width timing. The performance of a thruster is characterized by its nominal thrust, thrust repetitiveness, and response time, which is the time needed for the thrust to rise from 0 to 90 percent of its nominal value. These parameters determine how fast and how accurately the ASAT Kill Vehicle (KV) can put itself on a collision course with the target. In an idealized case all these parameters are assumed to function as required.

In real-world PNG-based ASAT all the systems function with a certain lag. Latencies in the seeker measurements and latencies in applying the acceleration command are two dominant factors that affect the intercept capability of the guidance system. These latencies will cause a significant miss distance, which would not take place if there were no latencies. The first two simulations are for an ideal system that does not include these factors. If Iran is not able to obtain an intercept even under these highly idealized conditions then it would not be able to do so using a system which has lags and imperfections built into it. The third simulation involves a real-world PNG-based ASAT missile.

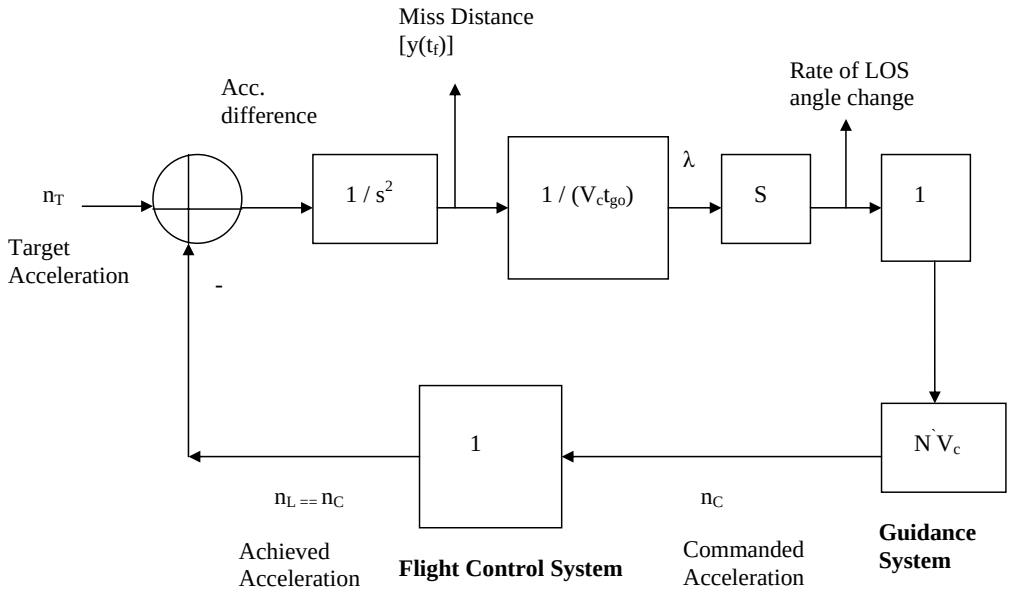

Figure 3.2: Ideal representation of PNG system

3.2.1 Simulation Case 1

For the first simulation run in the subroutine, the parameters for the guidance are mentioned in table 3.1.

Table 3.1: Guidance simulation parameters - Case 1

Horizontal separation	$107\ km$
Vertical separation	$107\ km$
Missile velocity	$8.53\ km/s$
Target satellite velocity	$7.35\ km/s$
Heading error (HE)	$0\ degrees$
Target accleration (nT)	$0\ G$

The horizontal and vertical separation distance between the missile and the target satellite is determined on the basis of the acquisition range that is obtained when the satellite is sunlit, which is the best possibility that an interceptor can have. For the first case the target acceleration and heading error are taken as zero. The simulation is run for three values of Navigation ratio ($N^{'}$), $N^{'} = [3, 4, 5]$ and for different values of update time, H (the time between each detector measurements). The final miss distance varies with

the update time H and is shown in table 3.2. The intercept geometry, closing velocity, commanded acceleration and miss distance during the intercept are shown in the figures 3.3, 3.4, 3.5 and 3.6 respectively. The sudden drop in closing velocity and the sudden rise in acceleration requirements are due to the missile and satellite crossing in space which causes a change in directional perspective.

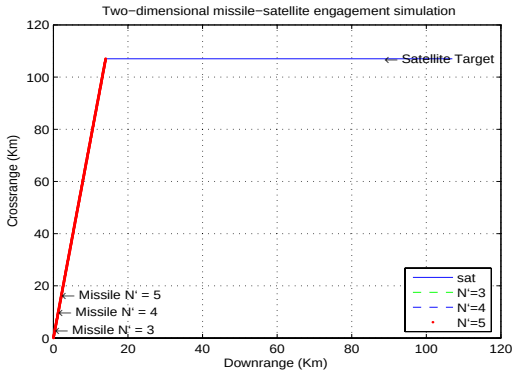

Figure 3.3: Case 1(H=0.02) Intercept Geometry

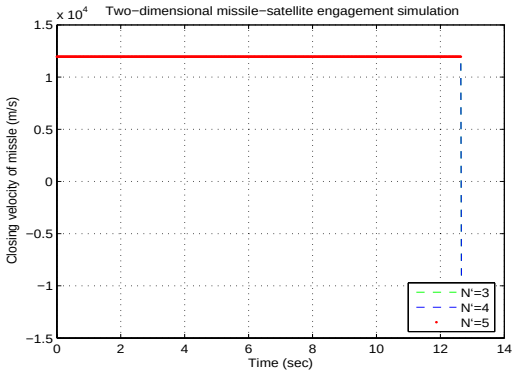

Figure 3.4: Case 1(H=0.02) Closing Velocity

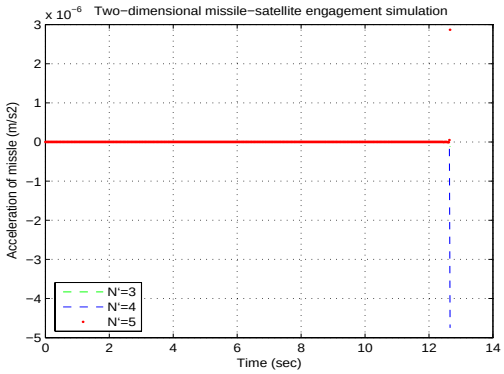

Figure 3.5: Case 1(H=0.02) Commanded acceleration for the interceptor

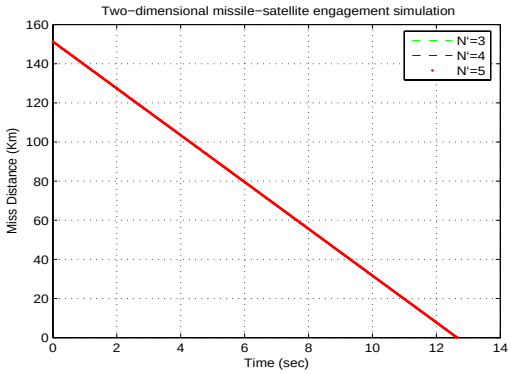

Figure 3.6: Case 1(H=0.02) Miss Distance at the end of each time step

3.2.2 Miss Distance for Various Update Intervals

As is seen from table 3.2, the miss distance varies hugely depending on the update interval (H). In the case of the candidate Iranian system, the

update interval is 50 Hz or one update per 0.02 seconds. For an update interval of H=0.02, the miss distance is nearly 110 meters, which is a complete failure of the intercept. For an update interval of H=0.002, the miss distance is 13 meters which is a substantial improvement in accuracy but still an intercept failure because a miss distance less than 1 meter is the requirement for a successful ASAT intercept in an head-on collision [2] [3]. Only when H=0.0002 (i.e. only when the Iranian system is fitted with a IR imaging system with 100 times more capability) is it able to make a successful intercept. But such an improvement in capability of the imaging system is a daunting engineering task. Improvement of this magnitude requires state of the art imaging systems that are available only to most technologically advanced establishments.

Table 3.2: Final miss distance

Upate Interval, H (sec)	**Navigation Constant**	**Miss Distance (Km)**
0.02	3	0.1084
0.02	4	0.1084
0.02	5	0.1084
0.002	3	0.0127
0.002	4	0.0127
0.002	5	0.0127
0.0002	3	0.0008
0.0002	4	0.0008
0.0002	5	0.0008

3.2.3 Simulation Case 2

For the second simulation run in the subroutine, the parameters for the guidance are in table 3.3. In this simulation case, the target acceleration is taken as 10G. The leading error is still assumed to be zero.

The simulation is run for three values of Navigation ratio ($N^{'}$), $N^{'} = [3, 4, 5]$ and for different values of update time, H (the time between each detector measurements). The final miss distance variation with the update time H is shown in table 3.4. The intercept geometry, closing velocity, commanded acceleration and miss distance during the intercept are shown in the figures 3.7, 3.8, 3.9 and 3.10 respectively.

Table 3.3: Guidance simulation parameters - Case 2

Horizontal separation	107 km
Vertical separation	107 km
Missile velocity	8.53 km/s
Target satellite velocity	7.35 km/s
Heading error (HE)	0 $degrees$
Target accleration (nT)	10 G

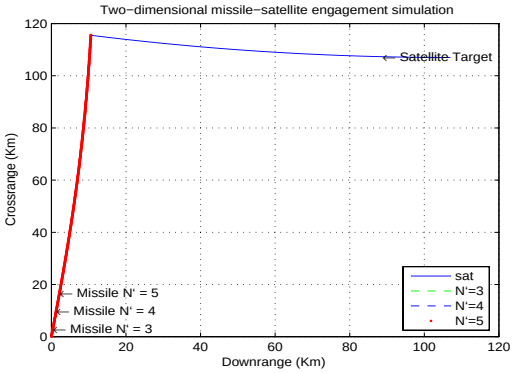

Figure 3.7: Case 2(H=0.02) Intercept Geometry

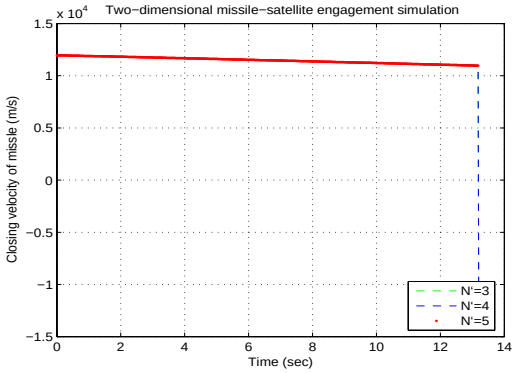

Figure 3.8: Case 2(H=0.02) Closing Velocity

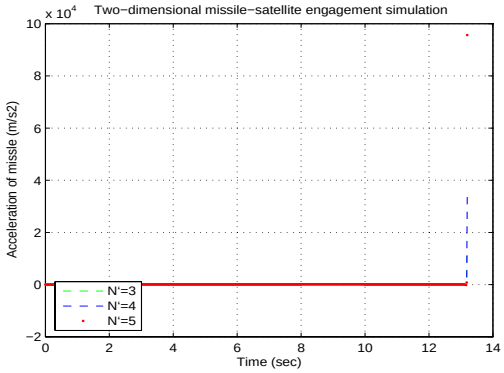

Figure 3.9: Case 2(H=0.02) Commanded acceleration for the interceptor

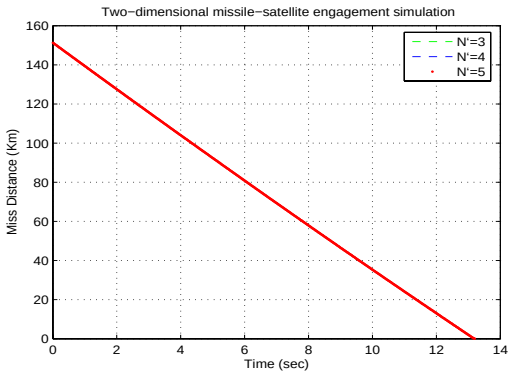

Figure 3.10: Case 2(H=0.02) Miss Distance at the end of each time step

3.2.4 Miss distance for various Update intervals

Similar to case 1, the miss distance varies with the update interval (H) for case 2 with $n_T = 10G$ as seen from table 3.4. In the case of the candidate Iranian system, the update interval is 50 Hz or one update per 0.02 seconds. For an update interval of H=0.02, the minimum miss distance is 120 meters which is a failure of the intercept. For an update interval of H=0.002 the minimum miss distance is 8 meters which is still larger than the requirement for a head-on collision. A miss distance less than 1 meter is the requirement for a successful ASAT intercept in a head-on collision [2] [3]. Only when H=0.0002 (i.e. only when the Iranian system is fitted with a IR imaging system with 100 times more capability) is the ASAT able to make a successful intercept. In that case, the minimum miss distance is 0.2 meters at N=3. Such an improvement of 100 times more imaging capability of the imaging system is not feasible without access to the most advanced imaging systems.

Table 3.4: Final miss distance

Upate Interval, H (sec)	**Navigation Constant**	**Miss Distance (Km)**
0.02	3	0.1204
0.02	4	0.1391
0.02	5	0.1492
0.002	3	0.0111
0.002	4	0.0078
0.002	5	0.0179
0.0002	3	0.0002
0.0002	4	0.0013
0.0002	5	0.0003

3.3 Simulation of a real-world PNG-based ASAT

In a real-world PNG based ASAT, it is assumed that all the systems in the anti-satellite (ASAT) missile function with a certain lag. Latencies in the seeker measurements and latencies in applying the acceleration command are two dominant factors that affect the intercept capability of the guidance system. These latencies will cause a significant miss distance, which would not take place if there were no latencies.

A binomial series representation of the guidance system dynamics provides an effective way of modelling a realistic PNG system. A representation of the system dynamics in the s domain is given by

$$\left(1+\frac{s\tau}{n}\right)^n = 1 + n\left(\frac{s\tau}{n}\right) + H.O.T \tag{3.26}$$

where τ is the guidance system time constant, n is the system order and H.O.T are higher order terms that can be neglected.

A fifth order system suitable for an analysis is shown in figure 3.11. This system allocates one time constant for the seeker, one for the noise filter and three for the flight control system. The transfer function for the system is

$$\frac{n_L}{\lambda} = \frac{N' V_c s}{\left(1+\frac{s\tau}{5}\right)^5} \tag{3.27}$$

The flight control system has a third-order representation to accommodate the autopilot and divert thrusters, which comprise the divert and attitude control system.

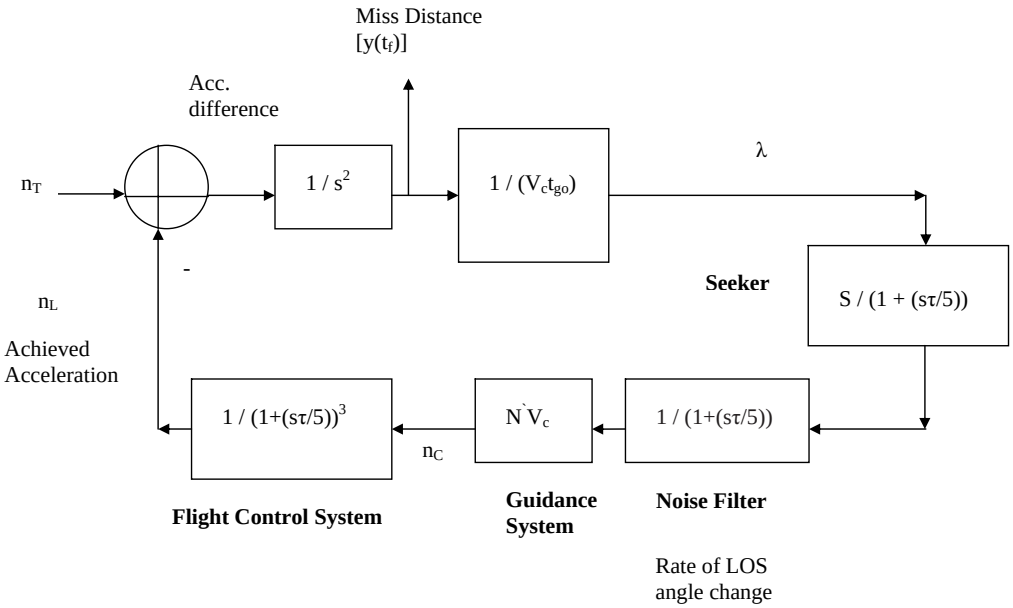

Figure 3.11: Fifth-Order representation of PN guidance system

3.3.1 Simulation Case 3

For the third simulation run in the subroutine the parameters for the guidance are as mentioned in table 3.3. But the guidance law is now a real-world non-ideal PNG law that has system lags.

Since this subroutine operates on the assumption of unbridled acceleration capability, there is no explicit possibility of an acceleration saturation occurring in the interceptor missile whereby the missile would lose fuel in mid-flight. This is an unrealistic assumption that needs to be corrected in further developments of this paper. The significance of this fact is shown in figure 3.13. However, it is observed from the simulation that the commanded acceleration requirements mount drastically in a real-world PNG guidance law based interceptor missile during the final stages of guidance.

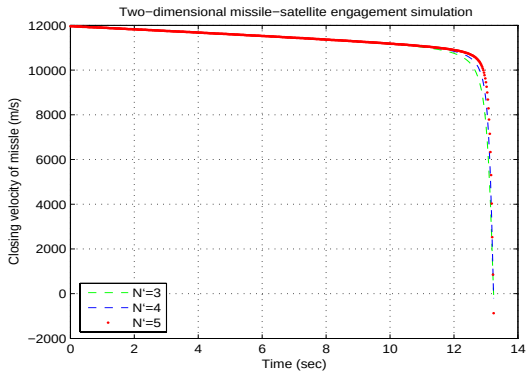

Figure 3.12: Case 3(H=0.02)
REAL-TIME PNG
Closing Velocity

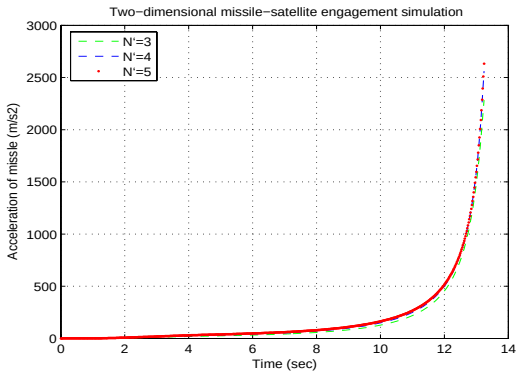

Figure 3.13: Case 3(H=0.02)
REAL-TIME PNG
Commanded Acceleration

By comparing figures 3.12 and 3.13 with figures 3.14 and 3.15 it is clearly observed that an real-time non-ideal PNG system has more demanding acceleration requirements that an ideal PNG system. This would lead to acceleration requirements for intercept of the missile reaching saturation limits and thus resulting in an intercept failure.

The effect of a real-world non-ideal PNG system is also felt on the final miss distance, as illustrated in table 3.5. We see from table 3.5 that for a real-world non-ideal PNG system the miss distances are too high to satisfy the limits of miss distance less than 1 meter.

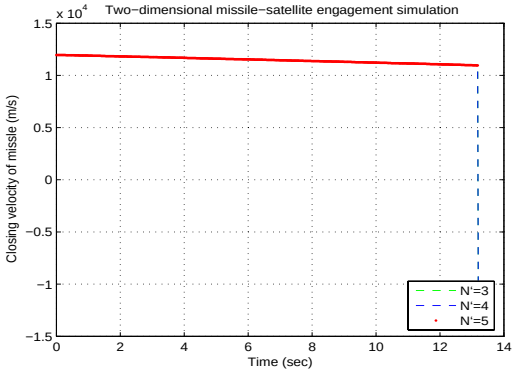

Figure 3.14: Case 2(H=0.02)
IDEAL PNG
Closing Velocity

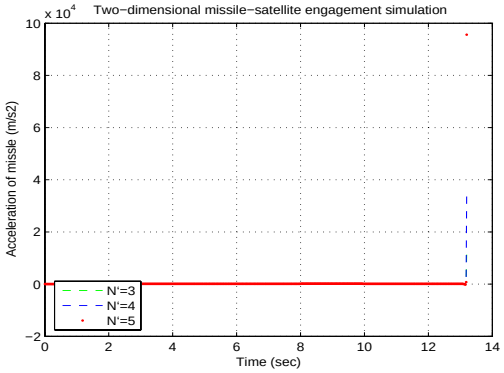

Figure 3.15: Case 2(H=0.02)
IDEAL PNG
Commanded Acceleration

Table 3.5: Final miss distance comparison (Ideal v. Real Time PNG Law)

PNG Law	**Upate Interval, H (sec)**	**Navigation Constant**	**Miss Distance (Km)**
Ideal	0.02	3	0.1204
Ideal	0.02	4	0.1391
Ideal	0.02	5	0.1492
RealWorld	0.02	3	2.3575
RealWorld	0.02	4	1.7095
RealWorld	0.02	5	1.2349

Chapter 4

Conclusion

This paper explores some of the technical difficulties that a country with a limited missile capability would face in developing a kinetic-energy ASAT capability. Such a capability requires an interceptor that can home with high accuracy and high speed on a satellite, which presents significant technical difficulties beyond those demonstrated in developing a limited missile capability. A country that possesses a limited missile capability therefore cannot be assumed to have the ability to field such an ASAT capability.

This paper has operated under certain assumptions whose effect on this judgement needs further exploration. Relaxing these assumptions is not expected to alter fundamentally the conclusion. First, the selected Proportional Navigation Guidance (PNG) law is the simplest to operate. There are other laws that are more accurate. PNG was chosen because it does not require anything as input apart from the distance between the missile and target. All other advanced laws require other inputs like closing velocity. This paper assumes that Iran does not have an advanced radar capability and cannot mount a radar seeker on its interceptor. If Iran is able to use an advanced radar or is able to mount an radar on its ASAT warhead, then Iran could used a better guidance law. The effect of such developments is left to future work. The second issue that needs further study is the various systemic effects of the real-time non-ideal fifth order PNG system. This would impose not only a large acceleration requirement on the missile but would also reduce the accuracy of the interceptor. These issues were not explored in detail in this paper and warrant further analysis.

Bibliography

[1] Ahmet Tarik Aydin. *Orbit Selection and EKV Guidance for Space-based ICBM Intercept.* Naval Postgraduate School, Monterey, California, USA. Spetember 2005.

[2] Florios Bardanis. *Kill Vehicle Effectiveness for Boost Phase Interception of Ballistic Missiles.* Naval Postgraduate School, Monterey, California, USA. June 2004.

[3] F. Smith et al. *Lightweight Exo-Atmospheric Projectile (LEAP) Space Test–LEAP 2 Flight.* AIAA 92-1070. 1992 Aerospace Design Conference, Irvine, CA.

[4] He Yingbo and Qiu Yong. *THAAD-Like high Altitude Theater Missile Defense: Strategic Defense Capability and Certain Countermeasures Analysis.* Science and Global Security, 11:151-202. Taylor and Francis Inc., 2003.

[5] Frank P. Incropera and David P. DeWitt. *Introduction to Heat Transfer.* Second Edition. John Wiley and sons, USA. 1990.

[6] John Lester Miller. *Principles of Infrared Technology. A practical guide to the the state of the art.* Van Nostrand Reinhold, New York, USA. 1994.

[7] NASA Imager for Magnetosphere-to-Aurora Global Exploration (IMAGE) satellite. Accessed online at http://image.gsfc.nasa.gov/poetry/workbook/page14.html.

[8] Paul Zarchan. *Tactical and Strategic Missile Guidance.* Progress in Astronautics and Aeronautics. A Volume in AIAA Tactital Missile Series. Fifth edition. AIAA, Virginia, US. 2007.

[9] *Weapons of Mass Destruction. WMD Around the World.* Federation of American Scientists (FAS). Accessed online at http://www.fas.org/nuke/guide/iran/missile/ on 12.10.2007.